



Friction Welding of Cast Iron and Phosphor Bronze

Anand K. Raghav¹ · R. Vaira Vignesh¹ · Kota Pavan Kalyan¹ · M. Govindaraju¹ 

Received: 10 July 2019 / Accepted: 23 December 2019 / Published online: 2 January 2020
© The Institution of Engineers (India) 2020

Abstract There is sometimes a need to fabricate machine parts that have the best properties of multiple materials while being economical at the same time. A prime example of such a scenario is with gears. Gears made out of cast iron are a poor choice because cast iron has poor impact resistance and is vulnerable to corrosion. The addition of phosphor bronze as an annulus to the cast iron hub in a composite gear provides the gear with those valuable resistances along with a superior intermeshing with mated gears. However, joining dissimilar materials such as cast iron to phosphor bronze is challenging when conventional welding techniques are employed. To overcome it, applying friction welding to join cast iron to phosphor bronze is focused in this thesis. The obtained results are analyzed and optimized for this particular combination of materials to facilitate their use in gears. The results show that there is an increased accumulation of graphite at the weld joints between cast iron and phosphor bronze for trials at higher (rotational) welding speeds, which leads to less favorable mechanical properties. At lower welding speeds, sound joints with acceptable mechanical and metallurgical properties were obtained.

Keywords Dissimilar welding · Friction welding · Cast iron · Phosphor bronze

Introduction

Friction welding is a solid-state joining process that can produce high-quality welds between two components with either similar or dissimilar chemical compositions. As the name suggests, the heat required to weld the two materials together is released from the frictional contact from forcing the materials to move against each other. At the point of contact, the materials get softened due to the heat produced. As the two softened materials move against each other, a weld is commenced. Once enough heat has been generated, the relative motion between the two materials is ended. To promote the solid-phase bond, a contact pressure is maintained or even increased for a specific period of time. The frictional welding process is performed by making use of a machine that converts mechanical energy to heat energy at the contact interface between the two materials by virtue of the relative motion between the two surfaces.

Cast iron is difficult to weld by conventional welding methods. However, Shinoda et al. [1, 2] described that friction welding mitigates the need of preheating of specimens for joining of gray cast iron and even nodular cast iron to other materials. Cheng et al. [3] calculated the thermal conduction as a function of the torque involved in the friction welding procedure. However, he noted that the torque is not usually calculated using a production friction welding machine and it is not easy to quantify the generation of heat in the process.

Wang and Nagappan [4] stated that the melted metal was squeezed out before melting starts, while they took the probability of melting at the interface into consideration in their numerical and analytical transient temperature study of welding AISI 1020 to steel. Their group inferred that there was a distinct variation in temperature response

✉ M. Govindaraju
m_govindaraju@ch.amrita.edu

¹ Department of Mechanical Engineering, Amrita School of Engineering, Coimbatore, Amrita Vishwa Vidyapeetham, Coimbatore, India

between continuous drive welding and inertial welding. In inertial welding, it was observed that the temperature gradient is much steeper compared to that in continuous drive friction welding. However, the peak temperatures in both inertial welding and continuous drive frictional welding were comparable to each other. The experimental results from Duffin and Bahrani [5] tend to downplay the possibility of melting at the interface between two substances with similar material compositions. For different materials, melting has been reported in a few cases, such as Al-SiC metal matrix composites to alloys of aluminum. Sahin [6] indicated that the temperature reaches its highest possible value far away from the middle of the weld interface, but not at the edge of the contact interface, noting that the heat transfer coefficient at the interface of the two work-pieces determines the location of these maxima.

Ma et al. [7] investigated the frictional welding of two dissimilar sheets of steel and conducted a detailed study of the mechanical and microstructural characteristics of the weld. Their findings clearly showed that the weld interface can be easily identified in the middle area, while the two welded metals undergo mechanical mixing along the edge of the weld. Nathan et al. [8] attempted to study the possibilities of utilizing titanium alloys for manufacturing the tools used for frictional stir welding along with the microstructural properties of the three tungsten-based alloy tools, with increasing purity of tungsten. The joint zone microstructure was observed by the scanning electron microscope and the chemical constitutions of the various compounds by energy-dispersive X-ray spectroscopy. The study found that the sample with the purest tungsten doped with 1% La₂O₃ displayed higher microstructural stability at increased temperatures during the frictional welding process.

A study was made by Savic et al. [9] in the joining of high-speed steel HS 6-5-2C to carbon steel C60, where a model of frictional welding of dissimilar metals was attempted, by observing the temperature cycles and the differences of the microstructure in the joining process. Studies of related natures [10–12] where the results which are related to structural and chemical variations in the welded joint were presented, along with the factors that influence welding parameters such as the shortening of joint deformation and joint radius. A study done by Padmanaban et al. [13] studied the effect that changing process parameters had on the strength of friction stir spot welding AA6061. Tensile shear failure was calculated for the aluminum alloy, and experiments were conducted for different variations of parameters such as tool rotational speed, shoulder diameter and friction dwell time. Vaira Vignesh et al. [14] conducted a study on the evolution of microstructure, hardness, and corrosion behavior friction stir processed of AA5083. The test results of Sujoy et al.

[15] and Ravikumar et al. [16] indicate that the peak temperature obtained in the course of friction stir welding process influences the weld nugget microstructure. Most of the available literature [13–19] investigates the development of joint and comprehends the microstructural evolution in the course of solid-state welding process of various metal alloy systems. However, a persistent literature gap exists on the joining of cast iron to phosphor bronze which is the critical need of most of the industries.

This research work aims to analyze the effects of the weld speed and configuration on the microstructural evolution microhardness, and joint strength between cast iron and phosphor bronze. The macrostructure and microstructure of the welded cross section were observed over the various configurations, and their variations were recorded. The tensile test and the microhardness survey of the welded joint were done in order to analyze the effect the rotational weld speed has on the process of friction welding cast iron and phosphor bronze.

Materials and Methodology

The base materials selected for this study are ASTM Grade 30 Gray Cast Iron and PB2 Phosphor Bronze. The material composition of these materials is shown in Tables 1 and 2. The mechanical properties of cast iron and phosphor bronze are displayed in Table 3.

The work-pieces of cast iron and phosphor bronze used in the inside out joint configuration are shown in Fig. 1. The variations in modeling the work-piece were to enable the weld in two different configurations—butt joint and inside out joint. The work-piece for the butt joint configuration has an indent on its surface with an outer diameter of 15 mm and an inner diameter of 13 mm, and a taper of 9° to the vertical. The work-piece for the inside out joint has a tapered hole through its length, with an outer diameter of 14 mm and an inner diameter of 13 mm. The length of the work-piece is 20 mm.

The vertical friction welding method was used to perform friction welding joints. The cast iron is maintained as the rotating part and the phosphor bronze is affixed to the bench as the stationary part in the process. The varying welding process trials are displayed in Table 4. In this experiment, frictional parameters such as frictional pressure, forging time, frictional time, and forging pressure are all kept constant with rotational speed being the sole

Table 1 Material composition of cast iron

C	Si	Mn	S	P	Fe
3.2%	2.3%	0.21%	0.02%	0.12%	Balance

Table 2 Material Composition of Phosphor Bronze

P	Sn	Zn	Ni	Pb	Fe	Cu
0.42%	11.4%	0.3%	0.5%	0.25%	0.15%	Balance

variable. The rotational speeds used in the experiment are 500 rpm, 710 rpm, and 1000 rpm. The different configurations and the welding parameters used in the friction welding trials are shown in Table 4.

The friction welding operations were carried out on a vertical frictional stir welding machine. In the present study, the only parameter of the vertical frictional stir welding machine which was changed was the rotational speed of the operation—for the purposes of the study, other parameters such as weld speed, forging pressure, and weld time were kept constant. Two different weld configurations were used in the study—the butt joint and the inside out joint. The three different weld speeds are used for both the configurations in the study.

The macro- and microstructures of the weld are examined for any defects that are observable to the naked eye, as well as under the optical microscope. Microstructural observations of the welded regions were conducted using both the optical microscope and the scanning electron microscope (SEM) under varying levels of magnification, at 50 times normal magnification, 100 times, 200 times, and 500 times normal magnification. These images of the weld zone were observed to study the variations in the microstructure of the weld zone at the various weld speeds and at the various configurations. Using standard metallography techniques, the cross sections of the welded joints are made ready for microstructural observation. The presence of intermetallic compounds and the accumulation of graphite at the weld interface were confirmed using EDS.

Table 4 Parameters of weld and weld configuration

S. no.	Welding configuration	Rotational welding speed
1	Butt joint	1000
2	Butt joint	1200
3	Butt joint	710
4	Inside out joint	710
5	Inside out joint	500

The microhardness survey was carried out at the weld interface of the joint between cast iron and phosphor bronze with a Vickers microhardness tester. A load of 0.2 kgf was applied by the tester to make an indent on the specimens, and the Vickers microhardness mapping for the welded cross section was performed. The friction welded tool and work-piece are machined and mounted on a universal testing machine (UTM) and subjected to tensile forces along the cumulative length of the tool and work-piece until tensile failure to determine the strength of the weld.

Results and Observations

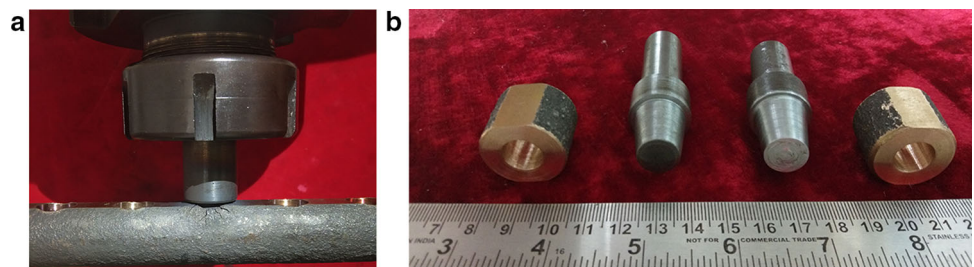
Macrostructure

The macroscopic observations of the weld have shown that the frictional weld between cast iron and phosphor bronze has been performed without any visual defects or cracks that are visible to the naked eye. Figure 2a shows the welded cross sections of the butt joint weld configuration at 1000 rpm, and Fig. 2b shows the welded cross section of the butt joint weld configuration at 710 rpm. Figure 3a shows the welded cross section of the inside out weld configuration at 710 rpm, and Fig. 3b shows the welded

Table 3 Material properties of cast iron and phosphor bronze

Material	Melting point (K)	α (K ⁻¹)	Density (g cm ⁻³)	Tensile strength (MPa)	Young’s modulus (GPa)
Cast Iron	1453–1653	11E–6	7.5	160	180
Phosphor Bronze	1193–1253	18E–6	8.8	450	110

Fig. 1 **a** Friction welding between cast iron and phosphor bronze in the butt joint configuration, **b** the cast iron tools and the phosphor bronze work-pieces that were used in the inside out configuration



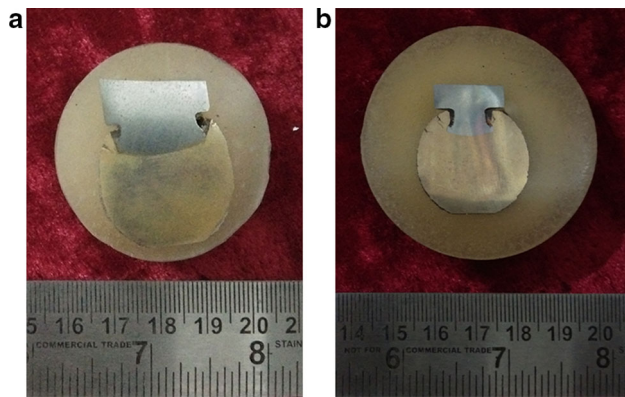


Fig. 2 Macrostructure images of the welded cross sections: **a** cross section of the friction weld in the butt joint configuration performed at 1000 rpm, **b** cross section of the friction weld in the butt joint configuration performed at 710 rpm

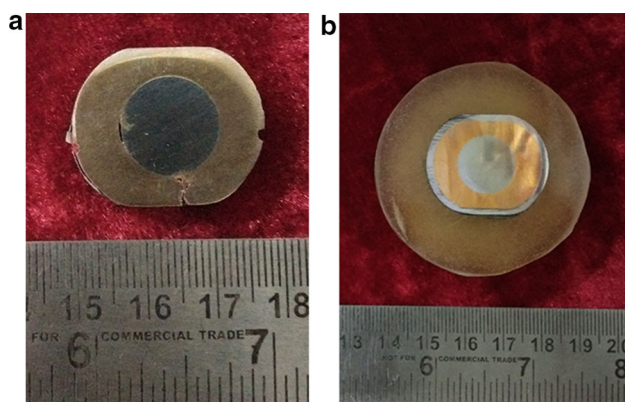


Fig. 3 Macrostructure of the welded cross sections: **a** cross section of the friction weld in the inside out joint configuration performed at 500 rpm, **b** cross section of the friction weld in the inside out configuration performed at 710 rpm

cross section of the inside out weld configuration at 500 rpm.

Microstructure

The microstructural evaluation of the welded joints through the optical microscope showed the presence of a plastic deformation zone and a heat-affected zone close to the weld interface. Differences in the physical and thermal properties of the welded materials in dissimilar metal welding resulted in asymmetrical deformation. In frictional welding, it is noted that the peripheral regions of the weld experience more heat generation compared to the central regions of the weld. Dynamic recrystallization causes the formation of finer grain size at the central regions of the weld [17]. The weld interface of the cast iron–phosphor bronze in the different weld configurations is shown in Fig. 4. The weld interface between cast iron and phosphor bronze is characterized by the accumulation of graphite at

the weld line, as shown in Fig. 5. This accumulation is found to increase with an increase in rotational welding speed of the operation.

With the utilization of elemental line mapping with EDS, it is clearly noted that there is a widespread accumulation of graphite at the weld boundary between gray cast iron and phosphor bronze. This accumulation is found to increase with an increase in the rotational welding speed of the friction welding trial. Figure 6 shows the elemental line mapping on the welded sample that confirms the increased graphite presence near the weld line.

Microhardness

The Vickers microhardness mapping was performed on the weld samples. The hardness mapping survey that was conducted across the CI-PB2 joint interface covering base material and abutting weld material affected by frictional heat is shown in Fig. 7. There is a tendency in the hardness results to be more analogous when moving away from the weld boundary. This is because of the higher frictional heat input generated from the inner parts of the weld, which results in a significant strain hardening effect. The peak hardness recorded at the CI-PB2 weld boundary can be attributed to the formation of the intermetallic compounds of cast iron and phosphor bronze along the joint line [18, 19]. The peak hardness measured in the weld zone was found to be 340 HV, which is significantly higher than the individual Vickers hardness values for either cast iron or phosphor bronze. The higher hardness values observed at the weld line is credited to the accumulation of graphite along the weld boundary. This behavior is again observed for samples welded in the butt joint configurations at both 1000 rpm and 710 rpm, along with the weld sample in the inside out weld configuration at 500 rpm. It is clearly observed from Fig. 7 that there is a sharp increase in the microhardness of the weld specimens at the weld boundary between cast iron and phosphor bronze.

Tensile Strength and Ductility

It was noted that the failures of all samples occurred on the welded joint from the cast iron side rather than the phosphor bronze side. The joint efficiency of the friction welded CI-PB2 joint was studied through tensile testing. The expected and desired strength of the weld is 40 MPa, which was achieved in the specimen welded at 710 rpm, as shown in Fig. 8. Corresponding elongation of the specimens is shown in Fig. 9. From the results, it is noted that the rotational speed of the frictional welding process is inversely proportional to the tensile strength of the welded joint. The duration of frictional welding time decides the amount of heat generated which is used for the softening of

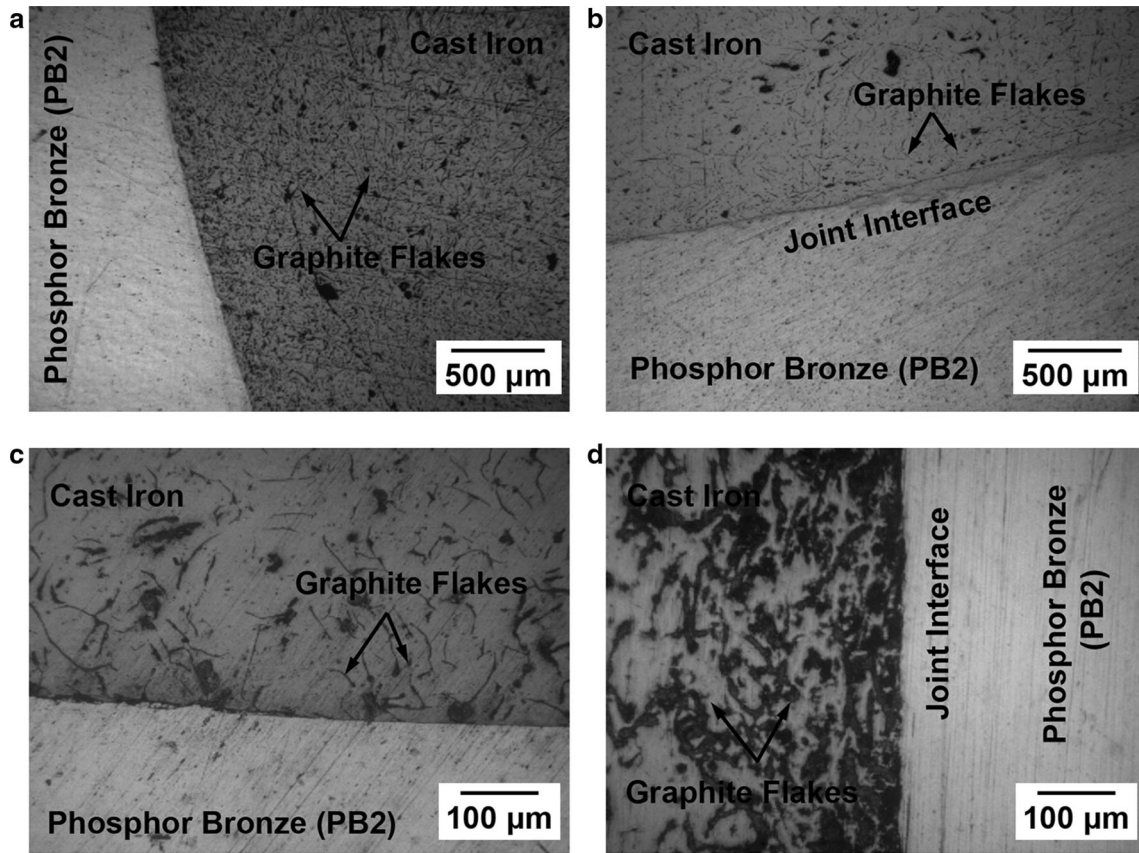


Fig. 4 Microstructure of the welded cross sections clearly show the accumulation of graphite towards the weld boundary

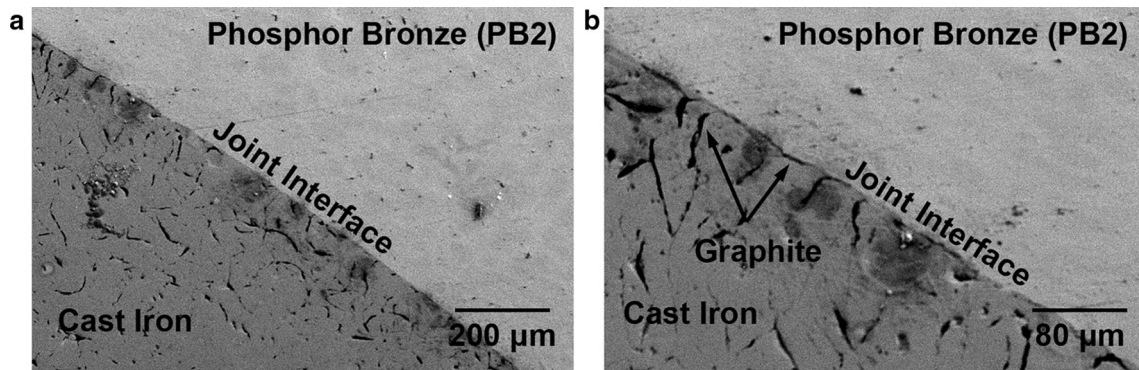


Fig. 5 Graphite accumulation at the weld boundary

metallurgical deformation and frictional welding. Through all the joints, the tensile failure occurred on the cast iron side. The tensile test results indicate that graphite accumulation leads to decreased strength at the weld joints and increased brittleness, which lead to failure at lower loads. At lower rotational weld speeds, however, the accumulation of graphite and the compression of the grain structure of cast iron and phosphor bronze are observed to be considerably lower, which leads to higher tensile strength for welds fabricated at those speeds. It is concluded that the

tensile strength of the weld increases with decrease in weld rotational speed.

Application of the Determined Process Parameters for Real-Time Component

The friction welding parameters that were obtained from the work were applied to weld real-time component made of cast iron and the phosphor bronze. A sound joint was developed between the cast iron and the phosphor bronze components, as shown in Fig. 10.

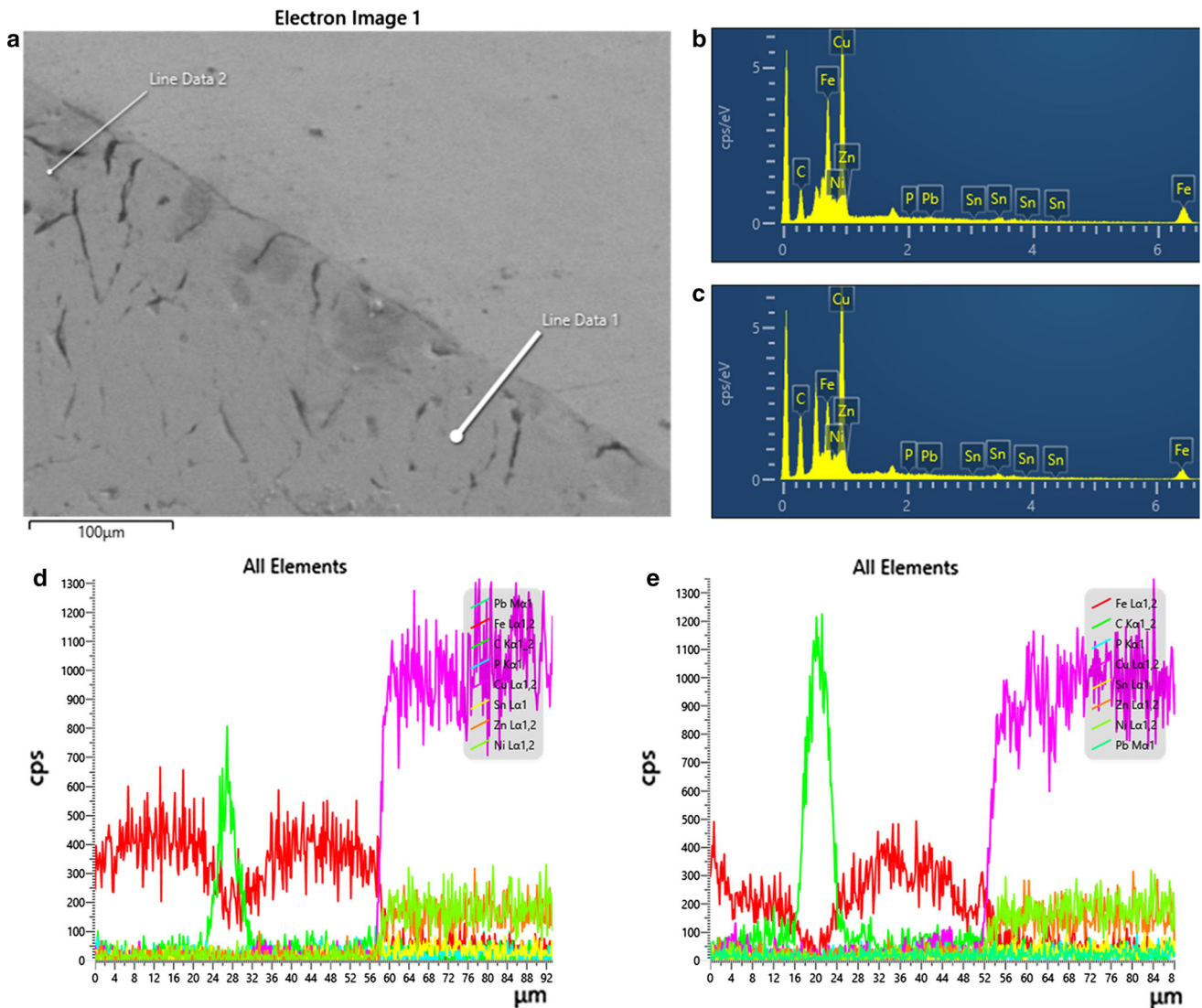


Fig. 6 a SEM image of the welded cross section. b, c Elemental composition of the weld boundary between cast iron and phosphor bronze. d, e Elemental line mapping of Line 1 and Line 2 of the weld boundary between cast iron and phosphor bronze

Conclusions

Friction welding runs between ASTM Grade 30 Gray Cast Iron and PB2 Phosphor Bronze was conducted, and their weld characterizations were analyzed and discussed. Also, the relation between the microstructure and the mechanical properties like hardness and tensile strength of the weld joint was examined and analyzed. The following conclusions were made:

1. The macro-structural images of the weld show that the weld between gray cast iron and phosphor bronze has been obtained without any visual defects.
2. Tensile strength of 40 MPa is the industrial requirement, which has been achieved at a lower rotational speed of 700 rpm.
3. A considerable increase in the microhardness is observed at the welded joint, due to possible work hardening of phosphor bronze by compressive load and accumulation of graphite from cast iron at the joint.
4. The rotational speed of frictional welding has a direct correlation with the accumulation of graphite at the welded joint. Microstructural analysis of the welded samples clearly displays the increased accumulation of graphite along the weld joint at higher rotational welding speeds. Therefore, higher speeds are not suitable for the process. At lower speeds, the accumulation of graphite is considerably less. This is in good agreement with tensile test results.

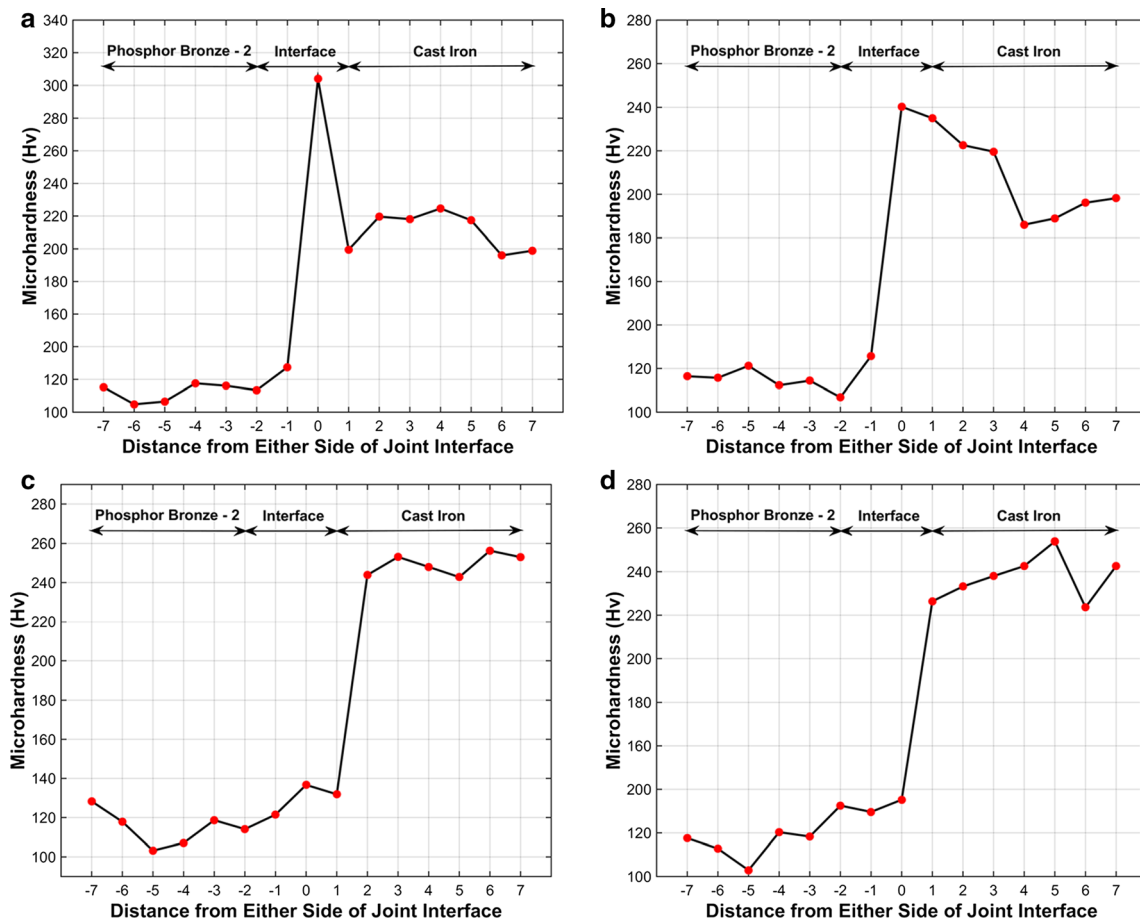


Fig. 7 Vickers microhardness mapping of **a** the inside out weld configuration at 710 rpm, **b** the inside out joint weld configuration at 500 rpm, **c** the butt joint weld configuration at 1000 rpm, **d** the butt joint weld configuration at 710 rpm

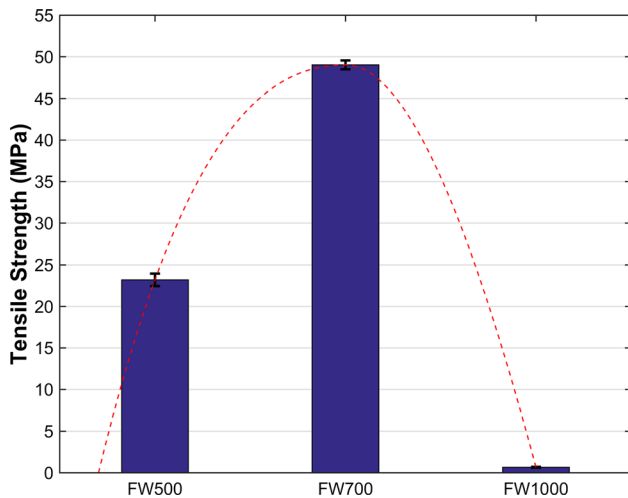


Fig. 8 Tensile Strengths of the various friction welding trials

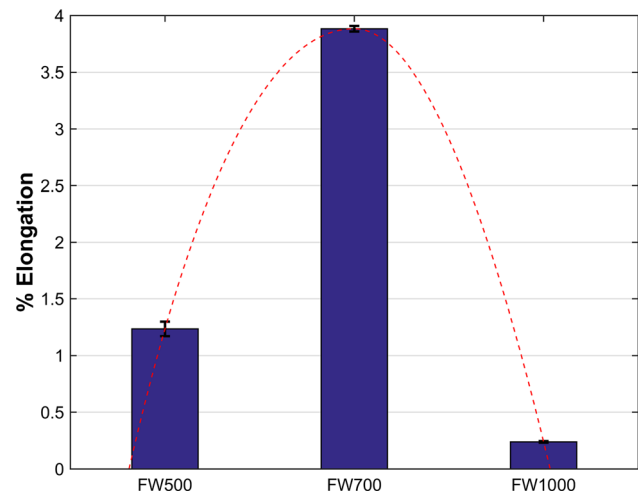


Fig. 9 Elongation percentages of the various friction welding trials

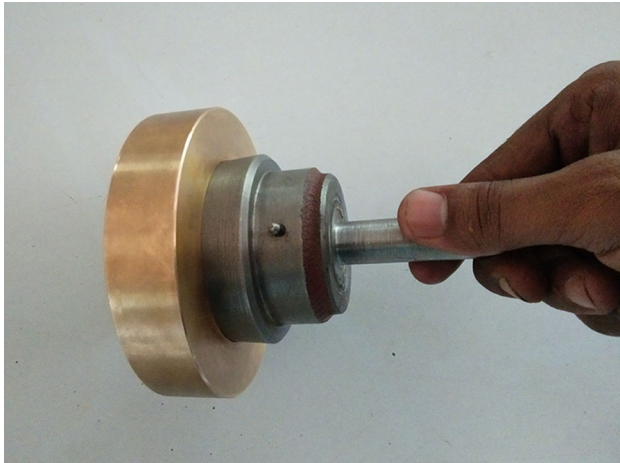


Fig. 10 Real-time friction welding operation between the cast iron and the phosphor bronze components were performed

- The future study may be oriented towards this phenomenon and fatigue properties of the joint, which are crucial for the application.

References

- T. Shinoda, H. Katsuei, Y. Ryouichi, Effect of friction welding parameters on mechanical properties of cast iron joints. *Q. J. Jpn. Weld. Soc.* **12**(3), 328–334 (1994)
- T. Shinoda, Recent topics of FSW technology in Japan. *Weld. World* **47**(11–12), 18–23 (2003)
- C.J. Cheng, Transient temperature distribution during friction welding of two similar materials in tubular form. *Weld. J.* **41**, 542–550s (1962)
- K.K. Wang, Transient temperature distribution in inertia welding of steels. *Weld. J.* **49**, 419s–426s (1970)
- F.D. Duffin, A.S. Bahrani, Frictional behaviour of mild steel in friction welding. *Wear* **26**(1), 53–74 (1973)
- M. Sahin, Joining of stainless-steel and aluminium materials by friction welding. *Int. J. Adv. Manuf. Technol.* **41**(5–6), 487–497 (2009)
- H. Ma, G. Qin, P. Geng, F. Li, B. Fu, X. Meng, Microstructure characterization and properties of carbon steel to stainless steel dissimilar metal joint made by friction welding. *Mater. Des.* **86**, 587–597 (2015)
- S.R. Nathan, V. Balasubramanian, S. Malarvizhi, A.G. Rao, An investigation on metallurgical characteristics of tungsten based tool materials used in friction stir welding of naval grade high strength low alloy steels. *Int. J. Refract. Met. Hard Mater.* **56**, 18–26 (2016)
- B. Savic, S. Markovic, R. Ciric, Physical model of the frictional welded joint of different types of steel. *FME Trans.* **36**(2), 93–97 (2008)
- N. Ratkovic, R. Nikolic, I. Samardzic, Structural, chemical and deformation changes in friction welded joint of dissimilar steels. *Metallurgy* **53**(4), 513–516 (2014)
- N. Ratkovic, A. Sedmak, M. Jovanovic, V. Lazic, R. Nikolic, B. Krstic, Physical and metallurgical changes during the frictional welding of the high-speed steel and the tempering steel. *Techn. Gaz.* **16**(3), 27–31 (2009)
- N. Ratkovic, D. Arsic, V. Lazic, R. Nikolic, B. Hadzima, The contact and compacting pressures influences on the quality of the friction welded joint. *Mater. Eng.* **23**(2), 51–57 (2016)
- R. Padmanaban, R. Vaira Vignesh, M. Arivarasu, A.A. Sundar, Process parameters effect on the strength of friction stir spot welded AA6061. *ARPN J. Eng. Appl. Sci.* **11**, 6030–6035 (2016)
- R. Vaira Vignesh, R. Padmanaban, M. Datta, Microstructure, hardness and corrosion behaviour of friction stir processed AA5083. *Anti-Corros. Methods Mater.* **66**(6), 791–801 (2019)
- S. Tikader, P.B.B. Puri, A study on tooling and its effect on heat generation and mechanical properties of welded joints in friction stir welding. *J. Inst. Eng. (India) Ser. C* **99**(2), 139–150 (2018)
- S. Ravikumar, V.S.J. Rao, Microstructural characterizations with EDAX analysis of dissimilar friction stir welds. *J. Inst. Eng. (India) Ser. C* **94**(4), 307–314 (2013)
- R. Jain, S.K. Pal, S.B. Singh, Finite element simulation of temperature and strain distribution during friction stir welding of AA2024 aluminum alloy. *J. Inst. Eng. (India) Ser. C* **98**(1), 37–43 (2017)
- B. Das, S. Pal, S. Bag, Monitoring of friction stir welding process using main spindle motor current. *J. Inst. Eng. (India) Ser. C* **99**(6), 711–716 (2018)
- R. Satish, V.S. Rao, D. Ananthapadmanaban, B. Ravi, Tensile strength and hardness correlations with microscopy in friction welded aluminium to copper. *J. Inst. Eng. (India) Ser. C* **97**(1), 121–126 (2016)

Publisher's Note Springer Nature remains neutral with regard to jurisdictional claims in published maps and institutional affiliations.